Molecules and Cells

Cell-Based Screen Using Amyloid Mimic β23 Expression Identifies Peucedanocoumarin III as a Novel Inhibitor of α-Synuclein and Huntingtin Aggregates

Sangwoo Ham[1], Hyojung Kim[1], Seojin Hwang[2], Hyunook Kang[3], Seung Pil Yun[4,5,6], Sangjune Kim[4,5,6], Donghoon Kim[4,5,6], Hyun Sook Kwon[7], Yun-Song Lee[1], MyoungLae Cho[7], Heung-Mook Shin[7], Heejung Choi[3], Ka Young Chung[8], Han Seok Ko[4,5,6], Gum Hwa Lee[2], and Yunjong Lee[1,9,*]

[1]Division of Pharmacology, Department of Molecular Cell Biology, Sungkyunkwan University School of Medicine, Suwon 16419, Korea, [2]College of Pharmacy, Chosun University, Gwangju 61452, Korea, [3]School of Biological Sciences, College of Natural Sciences, Seoul National University, Seoul 08826, Korea, [4]Neuroregeneration and Stem Cell Programs, Institute for Cell Engineering, [5]Department of Neurology, The Johns Hopkins University School of Medicine, Baltimore, MD 21205, USA, [6]Diana Helis Henry Medical Research Foundation, New Orleans, LA 70130, USA, [7]National Development Institute of Korean Medicine, Gyeongsan 38540, Korea, [8]School of Pharmacy, Sungkyunkwan University, Suwon 16419, Korea, [9]Samsung Medical Center, Sungkyunkwan University School of Medicine, Samsung Biomedical Research Institute, Seoul 06351, Korea
*Correspondence: ylee69@skku.edu
https://doi.org/10.14348/molcells.2019.0091
www.molcells.org

Aggregates of disease-causing proteins dysregulate cellular functions, thereby causing neuronal cell loss in diverse neurodegenerative diseases. Although many *in vitro* or *in vivo* studies of protein aggregate inhibitors have been performed, a therapeutic strategy to control aggregate toxicity has not been earnestly pursued, partly due to the limitations of available aggregate models. In this study, we established a tetracycline (Tet)-inducible nuclear aggregate (β23) expression model to screen potential lead compounds inhibiting β23-induced toxicity. High-throughput screening identified several natural compounds as nuclear β23 inhibitors, including peucedanocoumarin III (PCIII). Interestingly, PCIII accelerates disaggregation and proteasomal clearance of both nuclear and cytosolic β23 aggregates and protects SH-SY5Y cells from toxicity induced by β23 expression. Of translational relevance, PCIII disassembled fibrils and enhanced clearance of cytosolic and nuclear protein aggregates in cellular models of huntingtin and α-synuclein aggregation. Moreover, cellular toxicity was diminished with PCIII treatment for polyglutamine (PolyQ)-huntingtin expression and α-synuclein expression in conjunction with 6-hydroxydopamine (6-OHDA) treatment. Importantly, PCIII not only inhibited α-synuclein aggregation but also disaggregated preformed α-synuclein fibrils *in vitro*. Taken together, our results suggest that a Tet-Off β23 cell model could serve as a robust platform for screening effective lead compounds inhibiting nuclear or cytosolic protein aggregates. Brain-permeable PCIII or its derivatives could be beneficial for eliminating established protein aggregates.

Keywords: α-synuclein, amyloid, fibril, natural compound screen, neurodegenerative disease, peucedanocoumarin III, Tet-Off model

Received 7 May, 2019; revised 22 May, 2019; accepted 28 May, 2019; published online 15 June, 2019

eISSN: 0219-1032

INTRODUCTION

Dysregulation of intracellular protein homeostasis is associated with diverse neurodegenerative diseases (Ross and Poirier, 2004). The aggregation of disease-related proteins (i.e., α-synuclein, polyglutamine (polyQ) repeat expansion-containing huntingtin, TAR DNA-binding protein [TDP43]) can be increased by disease-linked mutations or environmental stresses, thereby affecting the viability of neuronal subtypes in many brain disorders (Brahmachari et al., 2016; Gorbatyuk et al., 2008; Landles and Bates, 2004; Mahul-Mellier et al., 2014; Scherzinger et al., 1997; Scotter et al., 2015; Spillantini and Goedert, 2000). Interestingly, amyloid-like aggregates of disease proteins, including α-synuclein, huntingtin, and TDP43, are localized in the cytoplasm and nucleus (Goers et al., 2003; Kontopoulos et al., 2006; Rousseaux et al., 2016; Scherzinger et al., 1997; Scotter et al., 2014; Wyttenbach et al., 2000), which suggests differential proteinopathic disruption of cellular functions. A recent study showed that cytoplasmic protein aggregates impair nucleo-cytoplasmic protein transport (Woerner et al., 2016), thereby causing robust cellular toxicity. Moreover, pathological nuclear α-synuclein (Goers et al., 2003; Kontopoulos et al., 2006; Rousseaux et al., 2016) and huntingtin (Cui et al., 2006) have been reported to alter gene transcription. Since both cytosolic and nuclear protein aggregates have detrimental effects on cellular function and viability, a therapeutic strategy to control aggregates in both compartments may be important for controlling pathological processes in neurodegenerative diseases, including Parkinson's disease (PD).

α-Synuclein is a major component of Lewy body inclusions in PD and other α-synucleinopathies (Norris et al., 2004; Spillantini and Goedert, 2000). Recently, pathologies of diseases related to α-synuclein oligomers or fibrils have been shown to propagate via neuron-to-neuron transmission (Luk et al., 2012; Mao et al., 2016). Several natural compounds have been identified and found to inhibit α-synuclein aggregation or convert toxic oligomer or fibril conformations into nontoxic species (Jha et al., 2016; Masuda et al., 2006; Singh et al., 2013). In most cases, *in vitro* α-synuclein incubation is used to monitor α-synuclein aggregation and screen potential inhibitors of α-synuclein toxicity. Indeed, thioflavin T-assisted assessments of amyloid formations have aided the identification of several compounds as α-synuclein inhibitors (e.g., Congo red and curcumin) (Masuda et al., 2006). Although this *in vitro* screening platform afforded investigation of a small number of compounds and their derivatives, it is low throughput and labor intensive, which hinders screening of large-scale compound libraries. Another weakness of this *in vitro* approach is that hit compounds may not have cell-protective functions or may have undesired toxicity profiles.

In this study, we established a tetracycline (Tet)-Off cell model expressing nuclear β-sheet amyloid aggregates (nuclear β23, as named in previous studies [Olzscha et al., 2011; Woerner et al., 2016]). β23 was initially developed to aid in the investigation molecular mechanisms of toxicity induced by disease-associated amyloid aggregates (Olzscha et al., 2011). β23 is an artificial protein designed to self-assemble into fibrils with repeated β strands of alternating patterns of polar and nonpolar residues (Olzscha et al., 2011). In the previous study, amyloid aggregate expression of β23 aided in the investigation of sequestration and dysregulation of functionally important endogenous proteins as molecular mechanisms of amyloid-induced cell toxicity (Olzscha et al., 2011). Using Tet-inducible expression and cellular toxicity as readouts, we identified several nuclear β23 inhibitors, including peucedanocoumarin III (PCIII). PCIII enhanced clearance of nuclear, as well as cytosolic, β23 aggregates and prevented the aggregation and toxicity of disease-related proteins (i.e., mutant huntingtin and α-synuclein). Significantly, *in vitro* analysis suggested that by facilitating disintegration of established pathological preformed fibrils (PFFs), PCIII could reverse toxicity mediated by intracellular protein inclusion.

MATERIALS AND METHODS

Chemicals and antibodies

The National Development Institute of Korean Medicine (NIKOM) provided the natural compound library, which contained 640 natural compounds of > 80% purity (1 mg/ml). This library was used for nuclear β23 inhibitor high-throughput screening. Natural compounds blocking β23 toxicity (i.e., PCIII, kaempferol-7-O-α-L-rhamnopyranoside, oregonin, and ophiocarpine) were extracted from herbal medications, purified, and validated using high-performance liquid chromatography (HPLC). Thioflavin S, Thioflavin T, 6-OHDA, doxycycline, Alamar blue, trypan blue, MG132, and carbobenzoxy-valyl-alanyl-aspartyl-[O-methyl]-fluoromethylketone (Z-VAD-FMK) were purchased from Sigma (USA). Doxorubicin was purchased from Selleck Chemicals. The primary antibodies used in this study were mouse antibody to hemagglutinin (HA) (12CA5, 1:1,000; Roche, Switzerland), mouse antibody to FLAG (M2, 1:5,000; Sigma), mouse antibody to α-synuclein (1:3,000; BD Transduction Laboratories, USA), rabbit antibody to green fluorescent protein (GFP) (cat# 2956, 1:5,000; Cell Signaling Technology, USA) mouse antibody to glyceraldehyde-3-phosphate dehydrogenase (GAPDH) (GT239, 1:5,000; GeneTex, USA), mouse antibody to poly (ADP-ribose) polymerase 1 (PARP1) (cat# 556494, 1:1,000; BD Bioscience, USA), conformation specific rabbit antibody to α-synuclein filaments (MJFR-14-6-4-2, cat# ab209538, 1:5,000; Abcam, USA) and horseradish peroxidase (HRP)-conjugated mouse antibody to β-actin (AC15; Sigma-Aldrich, USA). The secondary antibodies used were HRP-conjugated sheep antibody to mouse immunoglobulin G (IgG) (cat# RPN4301, 1:5,000; GE Healthcare, USA), HRP-conjugated donkey antibody to rabbit IgG (cat# RPN4101, 1:5,000; GE Healthcare), Alexa Fluor 488-conjugated donkey antibody to mouse IgG (H + L) (cat# A21202, 1:1,000; Invitrogen, USA), Alexa Fluor 568-conjugated donkey antibody to mouse IgG (cat# A10037, 1:1,000; Invitrogen), and Alexa Fluor 647-conjugated donkey antibody to mouse IgG (cat# A31571, 1:1,000; Invitrogen).

Plasmids

The double-strand oligos encoding nuclear β23, β23, and nuclear αS824 sequence were cloned into a pTRE-Dual2 plasmid (Clontech Laboratories, USA). The full sequence of

nuclear β23 with tags (NLS-FLAG-β23-HA) is as follows:

ATGCCAAAGAAGAAGCGGAAGGTCGGTTGCGACTACAAGGACGACGACGACAAGGGCATGCAGATCTCCATGGACTACAACATCCAGTTCCACAACAACGGCAACGAGATCCAGTTCGAGATCGACGACTCCGGCGGCGACATCGAGATCGAGATCCGGGGCCCCGGCGGCCGGGTGCACATCCAGCTGAACGACGGCCACGGCCACATCAAGGTGGACTTCAACAACGACGGCGGCGAGCTGCAGATCGACATGCACTACCCATACGACGTCCCAGACTACGCT.

The full DNA and amino acid sequence of β23 with tags (FLAG-β23-HA) is as follows:

ATGTGCGACTACAAGGACGACGACGACAAGGGCATGCAGATCTCCATGGACTACAACATCCAGTTCCACAACAACGGCAACGAGATCCAGTTCGAGATCGACGACTCCGGCGGCGACATCGAGATCGAGATCCGGGGCCCCGGCGGCCGGGTGCACATCCAGCTGAACGACGGCCACGGCCACATCAAGGTGGACTTCAACAACGACGGCGGCGAGCTGCAGATCGACATGCACTACCCATACGACGTCCCAGACTACGCTTAA;

MCDYKDDDDKGMQISMDYNIQFHNNGNEIQFEIDDSGGDIEIEIRGPGGRVHIQLNDGHGHIKVDFNNDGGELQIDMHYPYDVPDYA.

The full DNA and amino acid sequence of nuclear αS824 with tags (NLS-FLAG-αS824 -HA) is as follows:

ATGCCAAAGAAGAAGCGGAAGGTCGGTTGCGACTACAAGGACGACGACGACAAGGGCATGTACGGCAAGCTGAACGACCTGCTGGAGGACCTGCAGGAGGTGCTGAAGCACGTGAACCAGCACTGGCAGGGCGGCCAGAAGAACATGAACAAGGTGGACCACCACCTGCAGAACGTGATCGAGGACATCCACGACTTCATGCAGGGCGGCGGCTCCGGCGGCAAGCTGCAGGAGATGATGAAGGAGTTCCAGCAGGTGCTGGACGAGATCAAGCAGCAGCTGCAGGGCGGCGACAACTCCCTGCACAACGTGCACGAGAACATCAAGGAGATCTTCCACCACCTGGAGGAGCTGGTGCACCGGTACCCATACGACGTCCCAGACTACGCTTGA;

MPKKKRKVGCDYKDDDDKGMYGKLNDLLEDLQEVLKHVNQHWQGGQKNMNKVDHHLQNVIEDIHDFMQGGGSGGKLQEMMKEFQQVLDEIKQQLQGGDNSLHNVHENIKEIFHHLEELVHRYPYDVPDYA.

Construct integrity was verified by sequencing. Plasmid cytomegalovirus (pCMV)-tetracycline transactivator (tTA) was purchased from Clontech and the pTreTight-Htt94Q-CFP (Maynard et al., 2009) construct was purchased from Addgene in USA (Plasmid #23966). The HA-α-synuclein construct was generated as previously described (Brahmachari et al., 2016).

Purification of PCIII from *A. decursiva*

In March 2013, *A. decursiva* roots were purchased from a drug store in Gyeongsan, Gyeongbuk, Korea. The roots (8.0 kg) were extracted with 100% methanol (MeOH, 3 × 10 L) at room temperature. The extract (674.0 g) was evaporated using a vacuum rotary evaporator, and then suspended in H_2O (2 L) and solvent partitioned with dichloromethane (CH_2Cl_2, 2 L) and butanol (2 L). The CH_2Cl_2 fraction (212.0 g) was subjected to open column chromatography over silica gel (*n*-Hexane, ethyl-acetate from 1:0 to 0:1), which produced eleven fractions (A-K). Fraction E (10.1 g) was recrystallized from MeOH to yield solid PCIII (1.2 g).

HPLC-ELSD and NMR of PCIII

HPLC analysis was performed on an Agilent 1260 system, equipped with an evaporative light-scattering detector (ELSD) and a Kinetex C_{18} column (4.6 × 150 mm; Phenomenex, USA). The mobile phase consisted of 0.1% trifluoroacetic acid in water (v/v) (A) and acetonitrile (B). The injection volume was 3 μl and flow rate was kept at 0.5 ml/min for a total run time of 30 min. The gradient program was as follows: 2% (start, B), 5% (0-3 min, B), 100% (3-20 min, B), 2% (20-23 min, B), and kept at 2% (B) until the end of the run at 30 min. HPLC analysis found PCIII purity to be 99.9% (Fig. 1).

^{1}H and ^{13}C NMR spectra were recorded on a Jeol ECA-500 MHz NMR instrument, operating at 500 MHz for ^{1}H NMR and 125 MHz for ^{13}C NMR (JEOL, Japan) with tetramethylsilane as the internal standard. The PCIII structure observed was compared with that reported in previous literature (Chen et al., 1996; Takata et al., 1990).

PCIII: colorless needles; ESI-MS *m/z* 386; ^{1}H-NMR ($CDCl_3$, 500 MHz) δ 7.61 (1H, d, *J* = 9.5 Hz, H-4), 7.39 (1H, d, *J* = 8.6 Hz, H-5), 6.84 (1H, d, *J* = 8.6 Hz, H-6), 6.78 (1H, d, *J* = 7.0 Hz, H-3''), 6.24 (1H, d, *J* = 9.5 Hz, H-3), 6.23 (1H, d, *J* = 3.4 Hz, H-4'), 5.33 (1H, d, *J* = 3.4 Hz, H-3'), 2.09 (3H, s, OCO-CH_3), 1.84 (3H, s, H-5''), 1.76 (3H, d, *J* = 7.0 Hz, H-4''), 1.47 (3H, s, C-2'-CH_3), 1.39 (3H, s, C-2'-CH_3); ^{13}C-NMR ($CDCl_3$, 125 MHz) δ 169.3 (C-1'''), 166.3 (C-1''), 160.0 (C-2), 156.4 (C-7), 154.1 (C-9), 143.4 (C-4), 138.1 (C-3''), 129.1 (C-5), 127.9 (C-2''), 114.4 (C-6), 113.0 (C-3), 112.4 (C-10), 106.3 (C-8), 77.2 (C-2'), 71.1 (C-3'), 63.2 (C-4'), 23.7 (C-2'-CH_3), 23.5 (C-2'-CH_3), 20.5 (C-2'''), 14.3 (C-4''), 12.0 (C-5'')

Cell culture, transfection, and treatment

Human neuroblastoma SH-SY5Y cells (ATCC [American Type Culture Collection], USA) or HEK-293T cells were grown in DMEM containing 10% fetal bovine serum (FBS) (vol/vol) and antibiotics in a humidified 5% CO_2 atmosphere at 37°C. X-tremeGENE HP transfection reagent (Roche) was used for transient transfections according to the manufacturer's instructions. For α-synuclein PFF uptake experiments, SH-SY5Y cells were incubated for 4 days in complete media containing PFF (5 μg/ml). PFF was replaced every 2 days. SH-SY5Y cells were briefly washed with phosphate-buffered saline (PBS) and incubated in the presence of natural compounds for an indicated duration followed by western blot analysis of remnant PFF in cell lysates.

Subcellular fractionation

SH-SY5Y cells were fractionated into cytosol and nucleus fractions using the Qproteome Mitochondria Isolation Kit (Qiagen, Germany) according to manual instructions. Cytosolic fractions were further concentrated with acetone precipitation. The purity of each fraction was validated with western blots using antibodies to marker proteins for cytosolic (GAPDH, 2% of total cytosolic fraction) and nuclear (PARP1, 5% of total nuclear fraction) fractions.

Alamar blue-based high-throughput cell viability assay

As outlined in Figure 2C, HEK-293T cells were cotransfected with pCMV-tTA and TetP-nuclear β23 constructs. Cells were kept on doxycycline (200 ng/ml; Sigma)-containing complete

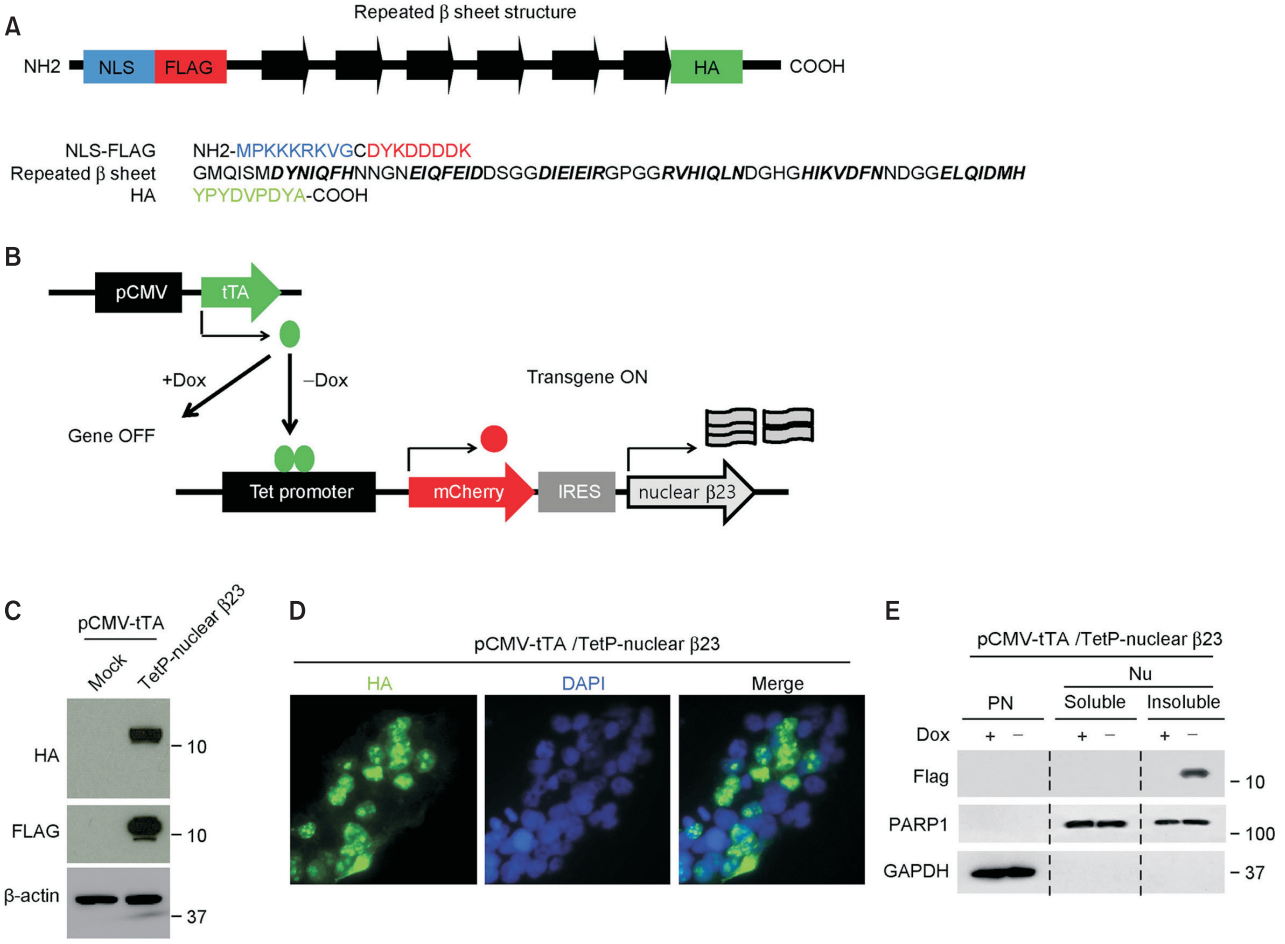

Fig. 1. Establishment of Tet-Off-inducible nuclear aggregation model. (A) Schematic structure of repeated β-sheet with an N-terminal NLS, FLAG tag and C-terminal influenza HA tag. The actual amino acid sequence for each structure is shown in the bottom panel. The repeated β-sheet structure is called β23 according to (Olzscha et al., 2011). (B) Illustration showing Tet-Off expression system of mCherry and nuclear β23 from TetP-NLS-FLAG-β23-HA (TetP-nuclear β23) construct when coexpressed with pCMV-tTA. Expression of mCherry and nuclear β23 is turned off by doxycycline binding to tTA, which causes conformational changes in tTA prohibiting it from binding to the Tet promoter. (C) Representative western blot with anti-HA and anti-FLAG antibodies showing nuclear β23 expression in HEK-293T cells cotransfected with pCMV-tTA and TetP-nuclear β23. β-Actin serves as a loading control. (D) Representative immunofluorescence images showing nuclear β23 expression in HEK-293T cells transfected with pCMV-tTA and pTetP-β23. Nuclear β23 was immunostained with anti-HA antibodies and the nucleus was counter-stained with DAPI. (E) Nuclear β23 distribution in the insoluble nuclear subcellular fraction of HEK-293T cells as determined by fractionation and subsequent western blots using anti-FLAG antibodies. GAPDH and Poly (ADP-ribose) polymerase 1 (PARP1) served as subcellular fraction markers of the post-nuclear (PN) and nuclear (Nu) compartments, respectively.

media to prevent toxic expression of nuclear β23. After 2 days, transfected HEK-293T cells were plated onto 96-well white flat-bottom plates (Microtiter; Thermo Scientific, USA) at 80% confluency in 100 μl of DMEM containing 10% FBS with penicillin/streptomycin (P/S) and without doxycycline for nuclear β23 induction. After 24 h, each compound (i.e., 640 natural compounds extracted and purified by NIKOM; 0.35 μg/ml each) was added to a well. For homogeneous treatment of each compound, 50 μl of culture media were removed and 50 μl of 2X compound in complete media were then added to each well. After 48 h incubation, cell viability was measured using Alamar blue assay. Briefly, 10 μl of filtered Alamar blue solution (1 mg/ml resazurin in DW filtered through a 0.22 μM pore filter) was added to the 100 μl culture media in 96-well plates. Cell viability was determined by fluorescence reading using a microplate fluorescence spectrometer (excitation: 530 nm, emission: 590 nm; SYNERGYneo microplate reader [BioTek, USA]). Each plate had four wells of the blank with no cell culture, positive controls (dimethyl sulfoxide [DMSO] vehicle treatment with β23 induction) and negative controls (no induction of β23 by maintaining in doxycycline [200 ng/ml]-containing media). To assess the appropriateness of our assay for high-throughput screening, the Z′ factor was quantified as follows:

Z′ factor = 1 – 3(SDp + SDn) / (MEANp – MEANn), where MEANp and MEANn are the means of the positive and nega-

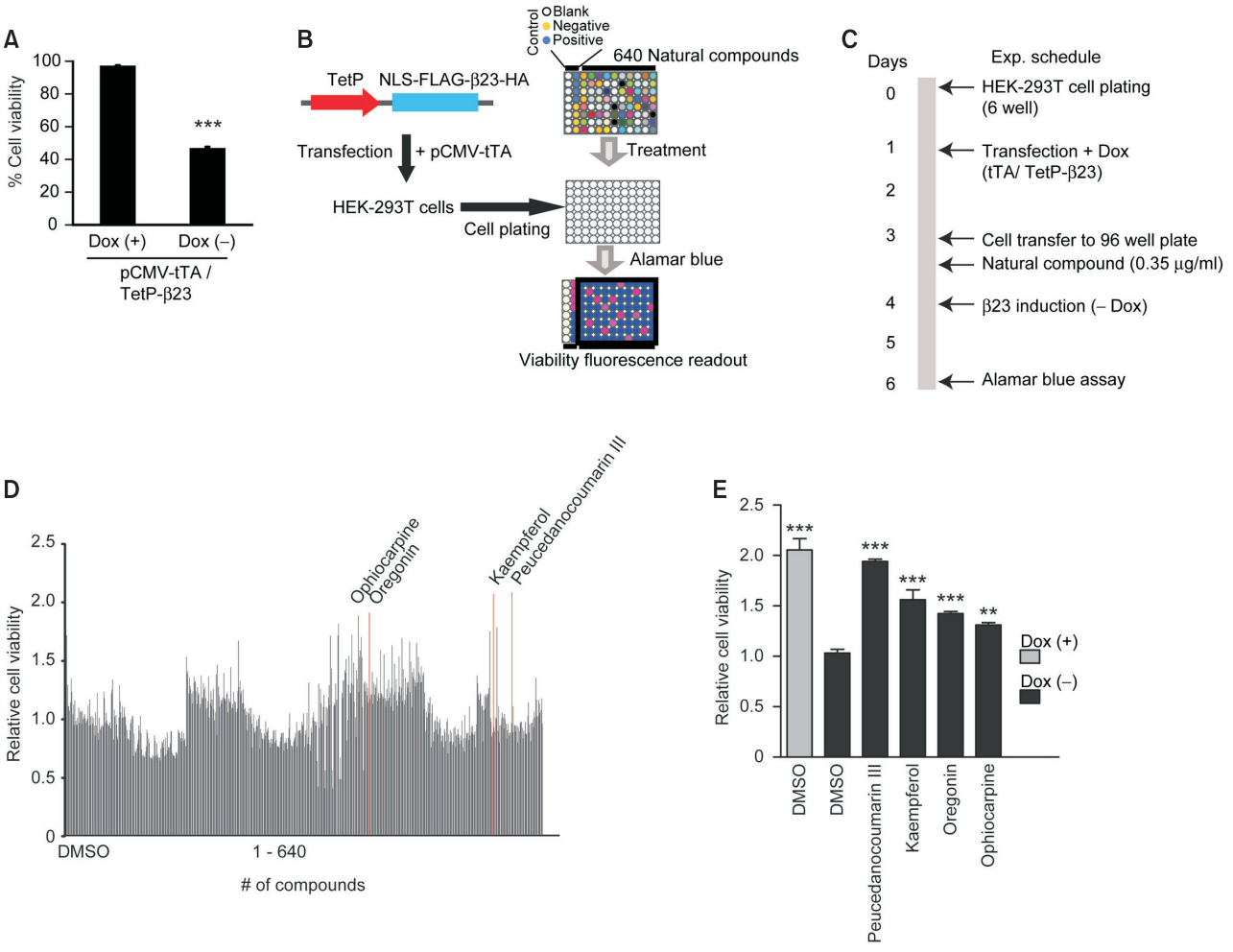

Fig. 2. High-throughput screen identifies nuclear β23 toxicity inhibitors. (A) Cell viability measured by Alamar blue fluorescence assay (n = 4) demonstrating cellular toxicity induced by 2 days of Tet-Off nuclear β23 aggregate expression in HEK-293T cells. (B) Schematic summary of high-throughput screening for natural compounds preventing toxicity induced by β23 expression in HEK-293T cells. HEK-293T cells transfected with pCMV-tTA and TetP-NLS-FLAG-β23-HA (TetP-β23) were treated with 640 natural compounds. Cell viability was assessed by Alamar blue fluorescence. For each plate, doxycycline treatment was a negative control and DMSO treatment was a positive control. (C) Detailed daily experimental (Exp.) schedule for high-throughput screening. (D) Initial high-throughput screening relative cell viability results determined by reading Alamar blue fluorescence. The top four ranked compounds are highlighted in red. (E) Quantification of the relative cell viability of hit compound-treated nuclear β23-expressing HEK-293T cells from the initial screening using Alamar blue assay (n = 6). The cell viability was normalized to the value of the DMSO positive control. Quantitative data are expressed as the mean ± SEM. Statistical significance was determined by unpaired two-tailed Student's *t*-test or ANOVA with Tukey *post-hoc* analysis. $^{**}P < 0.01$, $^{***}P < 0.001$.

tive controls, respectively, and SDp and SDn are the standard deviations of the positive and negative controls, respectively. A high-throughput screening-ready assay should have a Z′ factor between 0.5 and 1.

Western blot analysis

For Triton X-100-soluble and -insoluble fraction separation, SH-SY5Y cells were harvested and processed into nonionic detergent-soluble and detergent-insoluble fractions in lysis buffer containing PBS, 1% Triton X-100, Phosphatase Inhibitor Cocktail II and III (Sigma-Aldrich), and a complete protease inhibitor mixture. The lysates were centrifuged at 100,000*g* for 20 min at 4°C. The resulting pellet and supernatant (S1, soluble) fractions were collected. The pellet was washed once in lysis buffer containing nonionic detergent (1% Triton X-100) and solubilized in lysis buffer containing 1% SDS and 0.5% sodium deoxycholate. The homogenate was centrifuged and the resulting supernatant (nonionic detergent-insoluble) was collected. For total lysates, cells were harvested, washed twice with PBS, and lysed with Pierce RIPA buffer (150 mM NaCl, 50 mM Tris, pH 8.0, 1% NP40, 1% SDS, and 0.5% sodium deoxycholate, and a protease inhibitor mixture; Thermo Scientific) for 30 min on ice. Following this, cell lysates were prepared by centrifugation (22,250*g* at 4°C for 20

min). Protein concentration was determined using the Pierce™ BCA protein assay kit (Thermo Scientific). Equal amounts of protein (10-20 μg) were resolved on 8% to 16% SDS-PAGE and transferred to a nitrocellulose (NC) membrane. After washing with TBST (Tris-buffer solution-Tween20; 10 mM Tris-HCl [pH 7.6], 150 mM NaCl, and 0.05% Tween-20), membranes were blocked with 5% skim milk for 1 h and incubated with an appropriate primary antibody at the dilution recommended by the supplier. The membrane was then washed and primary antibodies were detected with HRP-conjugated secondary antibody. Immunoblot signals were visualized with Chemiluminescence (Pierce, USA). Densitometric analyses of immunoreactive bands were performed using NIH ImageJ software. The ratio between treated and control samples was calculated for each individual experiment and expressed relative to the control.

Fluorescence imaging

SH-SY5Y or HEK-293T cells were plated onto poly-D-lysine-coated coverslips at 10,000 cells/cm^2. Following experimental procedures, cells were fixed with 4% paraformaldehyde in PBS and blocked in a solution containing 5% normal donkey serum (Jackson ImmunoResearch, USA), 2% BSA (Sigma), and 0.1% Triton X-100 (Sigma) for 1 h at room temperature. Samples were then incubated overnight with corresponding primary antibodies against proteins of interest at 4°C. Briefly, cells grown on coverslips were washed with PBS containing 0.1% Triton X-100 and incubated for 1 h with fluorescence-conjugated secondary antibodies (1:500; Invitrogen) at room temperature. The coverslips were mounted with 4′, 6-diamidino-2-phenylindole (DAPI). Fluorescent images were obtained using a fluorescence microscope (Axiovert, 200 M; Carl Zeiss, Germany) or confocal microscope (TCS SP8 STED; Leica Microsystems, Germany) for four channel fluorescence image acquisition. For thioflavin S staining, thioflavin S (500 mM) was dissolved in 50% ethanol. Fixed SH-SY5Y cells were then stained with thioflavin S for 7 min. As a differentiation step to remove nonspecific binding of the dye, a slide was soaked in 100%, 95%, and 90% ethanol solutions for 10 s each and then transferred to PBS. Subsequent blocking and primary antibody binding steps were followed as described above for immunofluorescence staining.

Real-time quantitative polymerase chain reaction (PCR)

Total RNA was extracted with QIAzol Lysis Reagent (cat# 79306; Qiagen) and then treated with DNase I to eliminate trace DNA contamination. cDNA was synthesized from total RNA (1.5 μg) using a first-strand cDNA synthesis kit (iScript cDNA synthesis kit; Bio-Rad, USA). The relative quantities of β23 mRNA expression were analyzed using real-time PCR (QuantStudio 6 flex Real-Time PCR System; Applied Biosystems, USA). SYBR Green PCR master mix (cat# 4309155; Applied Biosystems) was used according to the manufacturer's instructions. The relative mRNA expression levels of β23 were calculated by the ΔΔCt method (Livak and Schmittgen, 2001) using GAPDH as an internal loading control. The primer sequences for real-time gene amplification are as follows:

hGAPDH: F- AAACCCATCACCATCTTCCAG, R- AGGGGCCATCCACAGTCTTCT;

β23: F- ATCTCGAGATGTGCGACTACAAGGACGAC, R-TACTCGAGTCAAGCGTAGTCTGGGACGTC.

Cell viability analysis

SH-SY5Y cells were plated in 6-well plates at a density of 0.5 × 10^6 cells per well. Following transient transfection with indicated constructs, cells were grown in DMEM containing low serum (2.5% FBS) for indicated days of α-synuclein, Tet-regulated β23, or mutant huntingtin (Htt94Q-CFP) expression. For α-synuclein toxicity, SH-SY5Y cells were treated with 6-OHDA or PBS vehicle control. SH-SY5Y cells were trypsinized to yield single-cell suspensions that were washed twice with PBS before resuspension in serum-free DMEM. Resuspended cells were mixed with an equal volume of 0.4% trypan blue (wt/vol) and incubated for 2 min at room temperature. Live and dead cells were analyzed automatically using the Countess II Automated Cell Counter (Life Technologies, USA). Cell Counting Kit-8 (CCK8) (Dojindo Molecular Technologies, USA) was also used to assess viability of HEK-293T cells by following the manufacturer's instructions.

Purification of recombinant protein, *in vitro* aggregation, and PFFs preparation

Plasmid pRK172-human α-synuclein was transformed to BL21-competent *Escherichia coli* by heat-shock transformation. Recombinant α-synuclein was induced and purified as previously described. Purified α-synuclein (100 μM) in the presence or absence of the PCIII was incubated in 1.5 ml EP tubes in sodium acetate buffer (100 mM, pH 7.5) at 37°C on a shaking incubator (300 rpm; Vision Scientific, Korea). At indicated days of incubation, EP tubes with protein solutions were subjected to fibril formation assessment using thioflavin T (100 μM; Sigma-Aldrich) fluorescence assay as reported previously. In each sample, thioflavin T binding and fluorescence were determined using a microplate fluorescence spectrometer (excitation: 450 nm, emission: 490 nm; SYNERGYneo microplate reader [BioTek]). For preparation of α-synuclein PFFs, α-synuclein fibrils (5 mg/ml) prepared from the 7 days incubation of monomeric α-synuclein were subjected to sonication (Vibra-Cell; Sonics & Materials, USA). Sixty pulses with 0.5 s duration of sonication power level 10% were applied with brief pause between every 10 pulses to prevent solution from heating up excessively. Quality of prepared PFF was validated by electron microscopy.

To investigate the disaggregating effects of PCIII against α-synuclein PFFs, α-synuclein fibrils (50 μM) prepared from the 7 days incubation of monomeric α-synuclein were subjected to *in vitro* incubation in sodium acetate buffer (100 mM, pH 7.5) with or without PCIII (100 μM) at 37°C on a shaking incubator (300 rpm; Vision Scientific). Samples were taken at 1, 3, and 7 days of incubation and subjected to thioflavin T fluorescence reading or western blot analysis.

Negative staining and transmission electron microscopy (TEM)

Recombinant human α-synuclein from *in vitro* reaction was applied to glow-discharged carbon-coated copper grids. After allowing the sample to absorb for 2 min and blotting off buffer solution onto Whatman paper, then the sample on the

grids were stained with 2% (w/v) uranyl acetate (UrAc) for 1 min. Then it was blotted off UrAc. TEM images were recorded at Korea Basic Science Institute (KBSI) with the Technai G_2 Spirit Twin microscope (FEI, USA) at an acceleration voltage of 120 kV.

Statistics

Quantitative data are presented as the mean ± standard error of the mean (SEM). Statistical significance was assessed with either an unpaired two-tailed Student's *t*-test for two-group comparisons or ANOVA with Tukey's honest significant difference *post-hoc* analysis for comparison of three or more groups. The results were considered significant at the level of $P < 0.05$.

RESULTS

Tet-Off expression of nuclear amyloid aggregates

To establish a cellular model of nuclear amyloid accumulation, we generated a Tet-Off construct capable of expressing artificial strands of β-sheet structure with an N-terminal nuclear localization sequence (NLS), FLAG tag and C-terminal influenza HA tag (Fig. 1A). In this manuscript, this construct is subsequently called nuclear β23, following previous studies in which β23's amyloid-like structure has been characterized (Olzscha et al., 2011; Woerner et al., 2016). Since β23 and reporter protein mCherry expression is under the control of a tetracycline-responsive promoter (TetP-β23), coexpression of a tTA is required for the activation of the Tet promoter and subsequent transcription of mCherry-internal ribosome entry site (IRES)-β23 (Fig. 1B). As designed, cotransfection with pCMV-tTA and TetP-nuclear β23 resulted in the expression of nuclear β23 and fluorescent reporter mCherry in HEK-293T cells (Fig. 1C, Supplementary Fig. S1A). Following subcellular fractionation, β23 expression was confined to the nucleus as determined by immunofluorescence and western blot experiments following subcellular fractionation (Fig. 1D, Supplementary Fig. S1B). To determine the solubility of β23, HEK-293T cells transfected with pCMV-tTA and TetP-nuclear β23 were fractionated into nuclear and post-nuclear compartments; and then the nuclear subcellular fraction was further separated into Triton X-soluble and -insoluble fractions. Western blot using FLAG tag antibodies demonstrated an exclusively insoluble β23 distribution in the nuclear fraction (Fig. 1E). Doxycycline successfully suppressed the induction of β23 aggregates (Fig. 1E).

Natural compound screening for novel inhibitors of nuclear aggregate toxicity

Following this, we assessed whether nuclear expression of amyloid β23 is toxic to HEK-293T cells. HEK-293T cells were transfected with pCMV-tTA and TetP-β23 constructs and incubated in complete media containing either doxycycline or vehicle as a control. In nuclear β23-expressing cells cultured for 2 days in the absence of doxycycline, cell viability measured by Alamar blue assay decreased to about 50% (Fig. 2A). Since the cell viability assay provided consistent and robust toxicity results, we used the Tet-Off nuclear β23 expression system to screen natural compounds that could potentially inhibit nuclear aggregate toxicity. For timed expression of β23, HEK-293T cells were transfected with pCMV-tTA and TetP-nuclear β23 and plated onto 96-well plates in the presence of doxycycline to suppress nuclear β23 expression (Figs. 2B and 2C). After plating, cells were treated with 640 natural compounds extracted and purified from clinically prescribed herbal medications (0.35 μg/ml). On the following day, nuclear β23 expression was induced by removing doxycycline. After 2 days of β23 induction, high-throughput cell viability was assessed by reading Alamar blue fluorescence (Fig. 2D). Z′ factors calculated for each plate using Alamar blue fluorescence intensities for negative (doxycycline treatment) and positive (no doxycycline + DMSO vehicle) controls were between 0.5 and 1.0 (Supplementary Fig. S2A), demonstrating that the experiment was robust, consistent, and appropriate for high-throughput screening. Initial screening identified several candidate nuclear β23 inhibitors (Fig. 2D) that increased cell viability against nuclear β23 toxicity. Repeated cell viability assay with the four most effective nuclear β23 inhibitors (i.e., PCIII, kaempferol-7-O-a-L-rhamnopyranoside, oregonin, and ophiocarpine) from the initial screen confirmed significant protective effects conferred by treatment with these compounds (Fig. 2E). A similar cytoprotective effect of nuclear β23 inhibitors was observed in an independent CCK8-based cell viability assessment (Supplementary Figs. S2B-D). These β23 inhibitors have diverse chemical structures (Supplementary Fig. S2E). Of these compounds, PCIII with a coumarin chemical backbone provided almost complete protection against β23-induced toxicity, resulting in cell viability comparable to doxycycline negative controls lacking β23 expression.

To determine whether cell death inhibition by these novel compounds is rather selective against toxic protein aggregation, an additional toxic insult (doxorubicin) was introduced into HEK-293T cells; after which, the cytoprotective effect of β23 inhibitors was examined (Supplementary Fig. S2F). Consistent with the report that doxorubicin induces apoptotic cell death via caspase activation (Gamen et al., 2000), the pan-caspase inhibitor Z-VAD substantially blocked doxorubicin-induced cell death (Supplementary Fig. S2G). However, all β23 inhibitors failed to prevent doxorubicin-induced cell toxicity (Supplementary Fig. S2G).

PCIII prevents amyloid aggregate toxicity

To assess the potential central nervous system applications for inhibitors of nuclear protein aggregation toxicity, we used the SH-SY5Y neuroblastoma cell line to examine the cytoprotective functions of select compounds. Transient transfection with pCMV-tTA and TetP-nuclear β23 in SH-SY5Y cells led to the expression of nuclear amyloid β23 and reporter protein mCherry (Fig. 3A). Nuclear β23 expression for 24 h in SH-SY5Y cells resulted in approximately 80% cell toxicity (Fig. 3B). All compounds (PCIII, kaempferol, oregonin, and ophiocarpine) increased SH-SY5Y cell viability against nuclear β23 induction, with PCIII providing maximal protection (up to 60% cell viability; Fig. 3B). Following this, we investigated whether these compounds improved cell viability against nuclear β23 toxicity through the alteration of protein aggregate clearance. To monitor β23 clearance over time, SH-SY5Y cells were transfected with pCMV-tTA and TetP-nuclear β23

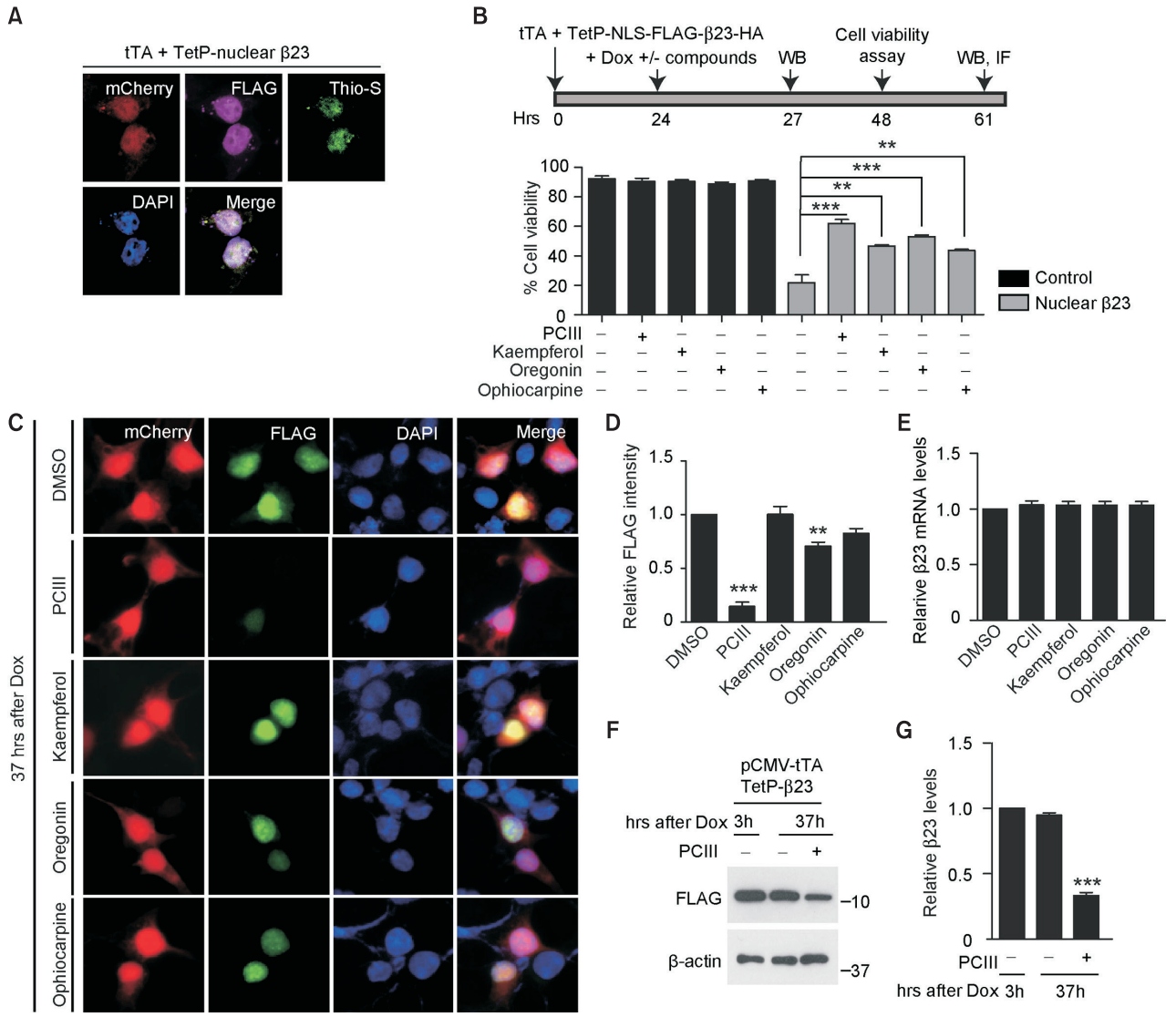

Fig. 3. PCIII prevents nuclear β23-induced toxicity by facilitating aggregate clearance. (A) Nuclear expression of β23 in SH-SY5Y cells transfected with pCMV-tTA and TetP-NLS-FLAG-β23-HA (TetP-nuclear β23) determined by immunofluorescence using FLAG antibodies. The amyloid structure was stained with thioflavin-S (Thio-S). Reporter protein mCherry was also expressed and the nucleus was counterstained with DAPI. (B) Experimental schedule used to monitor the degradation and toxicity of Tet-Off-expressed β23 (top panel). Cell viability measured by trypan blue exclusion assay (n = 6) showing the protective effect of natural compound treatments (1 μM each) in nuclear β23-expressing (48 h) SH-SY5Y cells transfected with pCMV-tTA and TetP-β23. Dox, doxycycline; WB, western blot; TB, trypan blue viability assay; IF, immunofluorescence. (C) Representative immunofluorescence images of FLAG (β23) and reporter protein mCherry in SH-SY5Y cells at 37 h after doxycycline treatment with or without natural compound cotreatment (1 μM). Doxycycline was added 24 h after pCMV-tTA and TetP-β23 transfection to stop further transcription of mCherry and β23. (D) Quantification of relative nuclear FLAG (β23) immunofluorescence intensities in the indicated experimental groups (n = 23 DMSO cells, 28 PCIII cells, 31 kaempferol cells, 37 oregonin cells, and 22 ophiocarpine cells from 2 independent experiments). (E) Quantification of relative β23 mRNA levels in SH-SY5Y cells transiently transfected with pCMV-tTA and TetP-nuclear β23 and treated with the indicated compounds (37 h), determined by real-time quantitative PCR (n = 3 per group). GAPDH mRNA levels were used as an internal loading control. (F) Representative western blot of nuclear β23 at indicated time points in SH-SY5Y cells treated with either PCIII or vehicle. β23 clearance was monitored using anti-FLAG antibodies. β-Actin served as a loading control. (G) Quantification of relative nuclear β23 protein levels normalized to β-actin for the indicated experimental groups (n = 3 per group). Quantitative data are expressed as the mean ± SEM. Statistical significance was determined by ANOVA with Tukey *post-hoc* analysis. $^{**}P < 0.01$, $^{***}P < 0.001$.

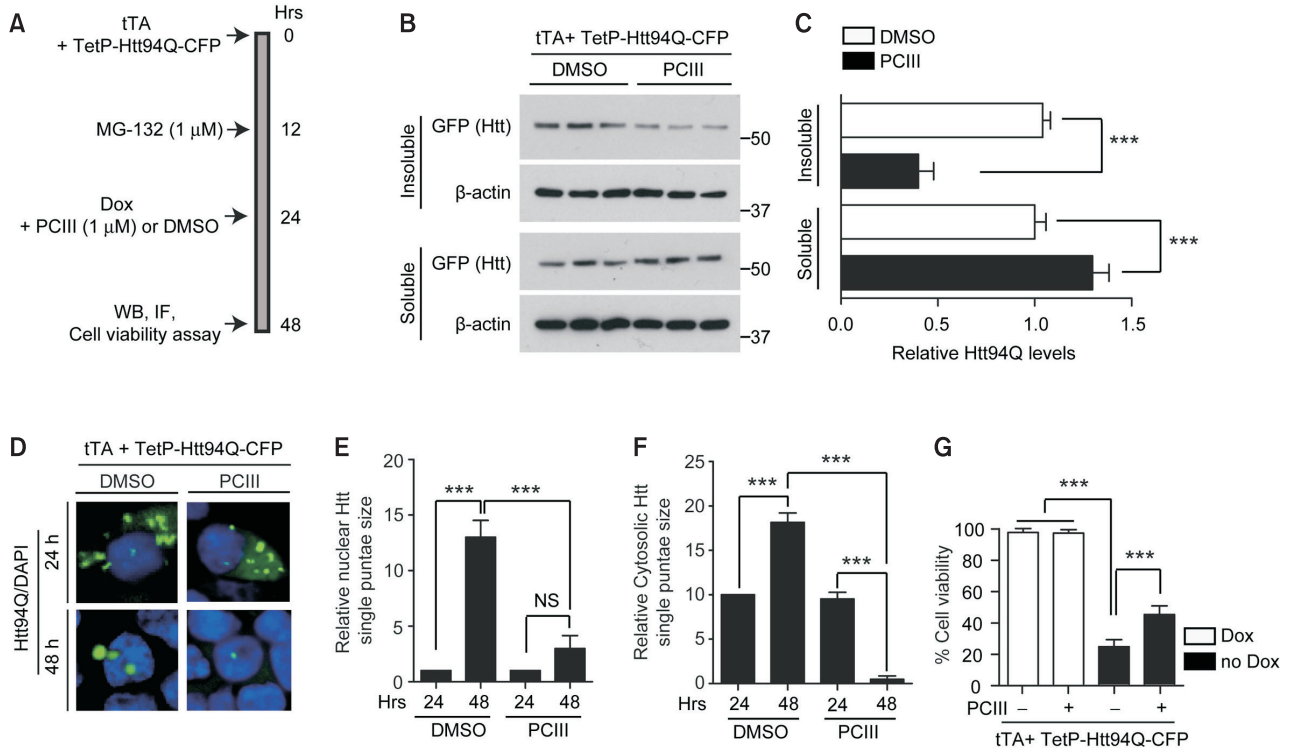

Fig. 4. PCIII suppresses mutant huntingtin aggregation and toxicity. (A) Diagram of the experimental schedule. SH-SY5Y cells were transiently transfected with pCMV-tTA and 94 polyglutamine repeat-containing huntingtin protein (pTetP-Htt94Q-CFP) constructs (24 h expression). Further Htt expression in SH-SY5Y cells was stopped by changing to doxycycline-containing media. Proteasome inhibitor MG132 (1 μM, 12 h) was added to induce nuclear Htt aggregate formation. After Htt expression was turned off by doxycycline, PCIII (1 μM) or vehicle were added to the culture media. Biochemical experiments and trypan blue cell viability assay were performed 48 h after transfection. WB, western blot; IF, immunofluorescence. (B) Western blot analysis of cyan fluorescent protein (CFP)-tagged mutant huntingtin (polyQ 94 repeat, Htt94Q-CFP) using anti-GFP antibodies distributed between 1% Triton X-100-soluble and -insoluble fractions in SH-SY5Y cells treated with PCIII or vehicle. (C) Relative amounts of mutant huntingtin distributed in insoluble and soluble fractions normalized to the β-actin internal loading control (n = 3 per group). (D) Representative immunofluorescence of Htt94Q-CFP aggregates in SH-SY5Y cells with DAPI counterstaining of the nucleus. Representative Htt94Q-CFP fluorescence images were taken 24 h after Htt94Q-CFP expression. Moreover, Htt94Q removal was assessed at 24 h following the addition of doxycycline and DMSO or PCIII treatment (48 h after initial transfection). (E) Quantification of relative nuclear puncta size in the indicated experimental groups (n = 24 DMSO cells [24 h], 24 PCIII cells [24 h], 22 DMSO cells [48 h], and 26 PCIII cells [48 h] from 2 independent experiments). (F) Quantification of relative cytoplasmic puncta size in the indicated experimental groups (n = 24 DMSO cells [24 h], 20 PCIII cells [24 h], 19 DMSO cells [48 h], and 28 PCIII cells [48 h] from 2 independent experiments). (G) Cell viability measured by trypan blue exclusion assay (n = 6) demonstrating prevention of mutant huntingtin aggregate-induced toxicity by PCIII treatment (1 μM) in SH-SY5Y cells. Quantitative data are expressed as the mean ± SEM. Statistical significance was determined by ANOVA with Tukey *post-hoc* analysis. ***$P < 0.001$.

(Fig. 3B; top panel). Twenty-four hours after transfection, doxycycline was added to stop further β23 and mCherry transcription in SH-SY5Y cells, and β23 stability was assessed by immunofluorescence using anti-FLAG antibodies. Immunofluorescence showed that PCIII treatment markedly increased the removal of FLAG-tagged β23 from the nucleus, whereas β23 still remained in the vehicle treatment control for 37 h following the addition of doxycycline (Figs. 3C and 3D). To a lesser extent, oregonin facilitated the removal of nuclear FLAG-tagged β23 (Figs. 3C and 3D). In contrast, despite their cytoprotective ability, kaempferol and ophiocarpine had no effect on β23 degradation. These compounds had no effect on reporter protein expression and stability as shown by mCherry fluorescence intensity (Fig. 3C). Moreover, transcription of β23 mRNA was not altered by β23 inhibitors (Fig. 3E).

Regulation of the stability of nuclear β23 by PCIII was further determined by quantitative western blot. Immunoblot results showed no difference in β23 levels over time, which suggests that nuclear amyloid β23 was highly stable and resistant to degradation (Figs. 3F and 3G). Consistent with the immunofluorescence results, PCIII treatment led to approximately 70% degradation of β23 (Figs. 3F and 3G). Taken together, these results show that PCIII's inhibition of nuclear β23-induced toxicity correlates with its ability to accelerate the degradation of nuclear amyloid β23, which is otherwise highly stable and cannot be cleared via an intrinsic degradation machinery.

Afterwards, the mechanisms of PCIII-mediated nuclear β23

clearance in SH-SY5Y cells were elucidated. Tet-Off expression construct of β23 with no NLS sequence (TetP-β23) was generated to assess whether PCIII's cytoprotective effect on amyloid toxicity is specific to nuclear aggregates. SH-SY5Y cells were co-transfected with pCMV-tTA and TetP-β23 constructs. β23 was expressed for the initial 24 h and further expression was terminated by doxycycline treatment. Cell viability was assessed 24 h after doxycycline treatment. Expression of β23 amyloid in SH-SY5Y cells resulted in robust cell death which was largely prevented by PCIII treatment (Supplementary Fig. S3A). Immunofluorescence experiments showed that β23 was expressed in both the cytosol and nucleus and formed thioflavin S-positive amyloid aggregates, which were cleared by PCIII treatment (Supplementary Fig. S3B). Clearance of β23 by PCIII treatment was also confirmed by a western blot experiment (Supplementary Fig. S3C). This result indicates that PCIII can disaggregate amyloid structure and prevent cell toxicity induced by both cytosolic and nuclear aggregates.

Amyloid selectivity of PCIII-mediated protein degradation was examined by generating an artificial protein containing an alpha helix structure (αS824), following previous reports (Olzscha et al., 2011; Woerner et al., 2016). Tet-Off construct of αS824 was cloned with NLS and FLAG sequence in the N terminus and HA tag in the C terminus (TetP-nuclear αS824). In contrast to aggregate-forming β23, αS824 was distributed to the soluble fraction (Supplementary Fig. S3D) and its nuclear expression was not stained with amyloid-sensitive dye thioflavin S (Supplementary Fig. S3E). No cell toxicity was observed with αS824 expression in SH-SY5Y cells (Supplementary Fig. S3F). αS824 was gradually degraded over time, leading to an approximated 70% clearance at 37 h, compared to the levels at 3 h after doxycycline treatment (Supplementary Figs. S3G and S3H). PCIII had no effect on αS824 degradation (Supplementary Figs. S3G and S3H), suggesting relative selectivity of PCIII on amyloid disaggregation and clearance.

Next, amyloid clearance facilitated by PCIII was investigated. The proteasome inhibitor, MG132, was treated for 24 h during clearance of nuclear β23 or αS824 in the presence or absence of PCIII (Supplementary Fig. S3I). PCIII-enhanced β23 degradation was abolished by MG132 treatment (Supplementary Fig. S3J), indicating that β23 degradation by PCIII was via proteasomal pathway. PCIII independent αS824 degradation was also blocked by MG132 treatment (Supplementary Fig. S3K).

PCIII attenuates huntingtin aggregation and toxicity

Of the compounds that were cytoprotective against nuclear and cytosolic aggregates, PCIII demonstrated the greatest protective and disaggregative effects. PCIII extracted and purified from *Angelica decursiva* (Supplementary Figs. S4A and S4B) has a good therapeutic index since it is not toxic to SH-SY5Y cells at high concentrations (Supplementary Fig. S4C). Moreover, at concentrations as low as 1 μM, PCIII provided complete cellular protection against nuclear and cytosolic β23 toxicity (Fig. 2E). Therefore, we further investigated PCIII to understand the molecular mechanisms of PCIII-mediated β23 toxicity prevention and its potential clinical applications for disease-associated protein aggregation.

To determine PCIII's therapeutic effects on disease-associated proteins, we selected a cellular model of mutant huntingtin aggregation, which is linked to hyperkinetic movement disorders in humans, such as Huntington's disease (Scherzinger et al., 1997). To examine whether PCIII can regulate nuclear huntingtin aggregation in cells, we transfected SH-SY5Y cells with pCMV-tTA and 94 polyglutamine repeat-containing huntingtin protein (TetP-Htt94Q-CFP) to induce aggregate formation (Fig. 4A). A proteasome inhibitor (MG132) was added to facilitate nuclear aggregate formation as previously described (Maynard et al., 2009; Wyttenbach et al., 2000). Separation of protein lysates into detergent (1% Triton X-100)-soluble and -insoluble fractions demonstrated that PCIII treatment markedly prevented insolubility of mutant huntingtin aggregates and redistributed huntingtin into soluble fractions (Figs. 4B and 4C). Consistent with western blot results, immunofluorescence demonstrated that PCIII treatment of SH-SY5Y cells was associated with substantial removal of cytosolic and nuclear aggregate puncta formed because of Htt94Q expression (Figs. 4D-F). Moreover, the growth of mutant huntingtin aggregate size in DMSO-treated controls was inhibited or diminished by PCIII treatment in the nucleus and cytoplasm, respectively (Figs. 4E and 4F). Mutant huntingtin aggregate expression led to 80% cell death in SH-SY5Y cells; however, PCIII treatment improved cell viability by approximately 20% (Fig. 4G).

PCIII attenuates α-synuclein aggregation and toxicity

After observing the promising effects of PCIII on amyloid β23 and huntingtin aggregate toxicity, we tested PCIII's protective effects on pathological α-synuclein aggregates associated with PD. α-Synuclein was selected since its aggregates have been observed in the cytosol and nucleus (Goers et al., 2003; Gorbatyuk et al., 2008; Kontopoulos et al., 2006; Rousseaux et al., 2016). Moreover, the presence of α-synuclein aggregates in Lewy body inclusions characterizes a wide range of human brain disorders (Shults, 2006; Spillantini and Goedert, 2000). Since PCIII was able to enhance clearance of established nuclear amyloid structures (i.e., β23), we hypothesized that α-synuclein PFFs could also be modulated by PCIII. To test this possibility, HA-α-synuclein expressing SH-SY5Y cells were incubated with PFFs (5 μg/ml; Supplementary Fig. S5A) in media for 24 h to induce uptake of α-synuclein fibril seeds into the cytoplasm (Fig. 5A). Four days incubation of SH-SY5Y cells with PFFs established a cellular model of α-synuclein aggregate formation in both cytoplasm and the nucleus (Supplementary Fig. S5B) when determined by immunofluorescence imaging using fibril conformation specific anti-α-synuclein antibodies. Using this newly established SH-SY5Y cells with α-synuclein aggregate formation, intracellular PFF clearance was monitored by western blots of total protein lysates using conformation specific anti-α-synuclein fibril antibodies. Total protein lysates were prepared from SH-SY5Y cells at 0, 24, and 48 h following media change and the addition of PCIII or vehicle. The amount of high-molecular-weight α-synuclein fibril species strongly decreased with PCIII treatment compared with that reported for vehicle treatment (Figs. 5B and 5C). Accelerated clearance of α-synuclein aggregates by PCIII was further confirmed by immunofluo-

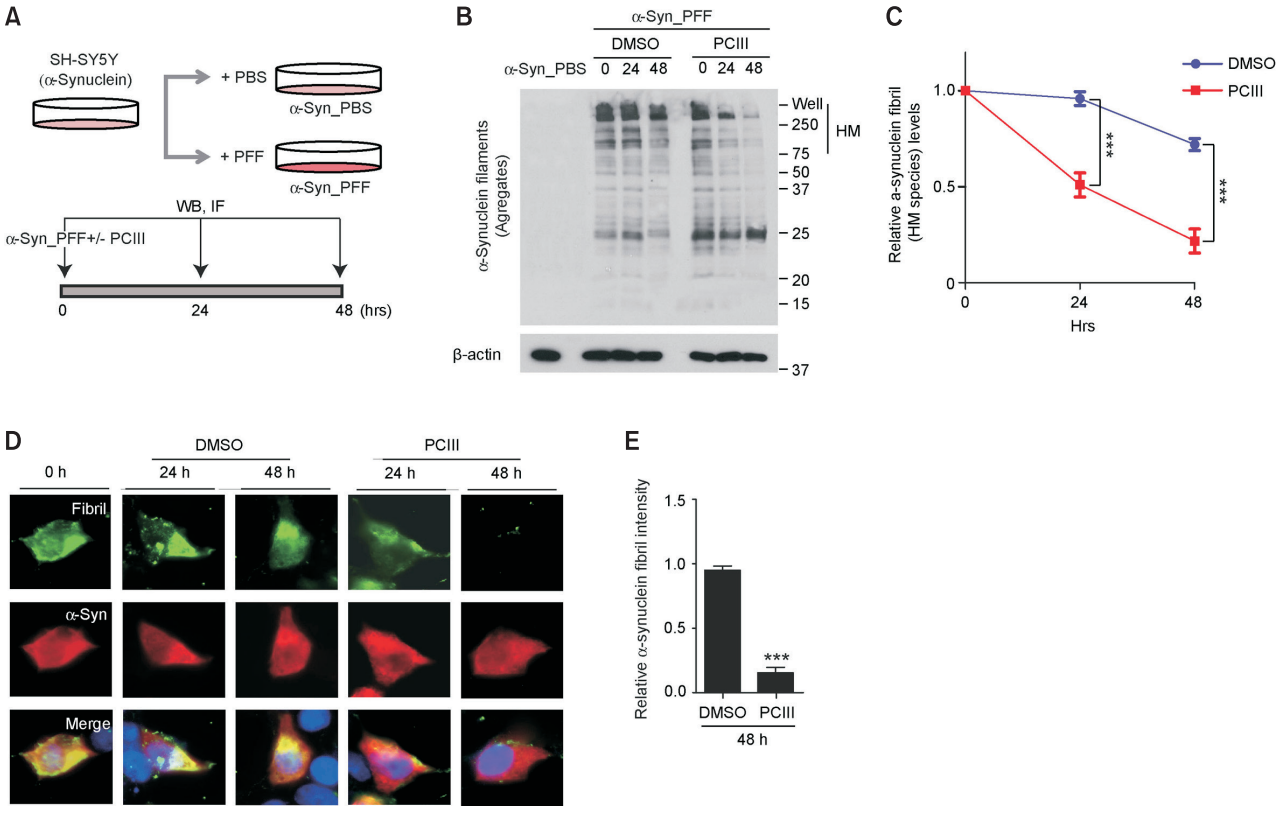

Fig. 5. PCIII disaggregates α-synuclein PFFs in SH-SY5Y cells. (A) Illustration of experimental procedure for establishment of intracellular α-synuclein fibril formation. Briefly, SH-SY5Y cells were transiently transfected with HA-α-synuclein construct (24 h). HA-α-synuclein expressing SH-SY5Y cells were treated with α-synuclein PFF (final concentration 5 μg/ml) or PBS as control every two day. Following 4 days of PFF uptake and brief wash, SH-SY5Y cells were subjected for PFF clearance assay with treatment of PCIII (1 μM) or DMSO as vehicle. WB, western blot; IF, immunofluorescence. (B) α-Synuclein PFF clearance in SH-SY5Y cells treated with PCIII (1 μM: 0 h, 24 h, 48 h) or vehicle at the indicated time points following PFF treatment determined by western blot using anti-α-synuclein filament specific antibodies. A PFF-untreated control sample (α-syn_PBS) with α-synuclein overexpression was included in the first lane. β-Actin served as an internal loading control. (C) Quantification of the relative amounts of high molecular weight (HM) α-synuclein fibrils for samples shown in panel A (n = 3 per group). (D) Representative immunofluorescence images of SH-SY5Y cells with α-synuclein PFF uptake using antibodies specific for α-synuclein (red) or fibril form of α-synuclein (green). Intracellular α-synuclein fibril in SH-SY5Y cells was monitored by immunostaining with α-synuclein fibril specific antibodies at the indicated time points (24 h and 48 h) after DMSO or PCIII (1 μM) treatment. (E) Quantification of the relative α-synuclein fibril intensities from immunofluorescence images obtained at 48 h following treatment of each compound (n = 31 DMSO cells, and 28 PCIII cells from two independent experiments. Normalized to signals from DMSO control sample.). Quantitative data are expressed as the mean ± SEM. Statistical significance was determined by unpaired two-tailed Student's *t*-test or ANOVA with Tukey *post-hoc* analysis. ***$P < 0.001$.

rescence using conformation specific α-synuclein fibril antibodies (Figs. 5D and 5E). PCIII treatment for 48 h decreased α-synuclein fibril intensities by approximate 80% compared to DMSO control (Fig. 5E).

In addition to the above mentioned cellular model of α-synuclein aggregation, toxin induced cellular PD model was also generated by treating HA-α-synuclein expressing SH-SY5Y cells with 6-OHDA to induce α-synuclein aggregation and toxicity (Supplementary Fig. S6A). Treatment of SH-SY5Y cells with 6-OHDA distributes α-synuclein into the Triton X-100-insoluble fraction in the nucleus subcellular compartment (Supplementary Figs. S6A and S6B). A 6-OHDA treatment-induced increase in nuclear α-synuclein insolubility was markedly attenuated by PCIII treatment (Supplementary Figs. S6A and S6B). Amyloid formation was assessed by thioflavin-S staining of HA-α-synuclein-expressing cells. Consistent with previous reports, thioflavin S-positive cytosolic aggregates increased substantially following 6-OHDA treatment (Supplementary Figs. S6C and S6D). PCIII treatment diminished thioflavin S signals, indicating that PCIII inhibits protein aggregates in the cytosol and nucleus. Trypan blue exclusion assay was used to assess the viability of SH-SY5Y cells against α-synuclein and 6-OHDA. The viability of α-synuclein-expressing SH-SY5Y cells decreased to 40% with 6-OHDA treatment and increased to 60% with PCIII treatment (Supplementary Fig. S6E). Taken together, these results show that PCIII prevents α-synuclein aggregation in the nucleus and cytosol, which may allow it to protect cells against α-synuclein

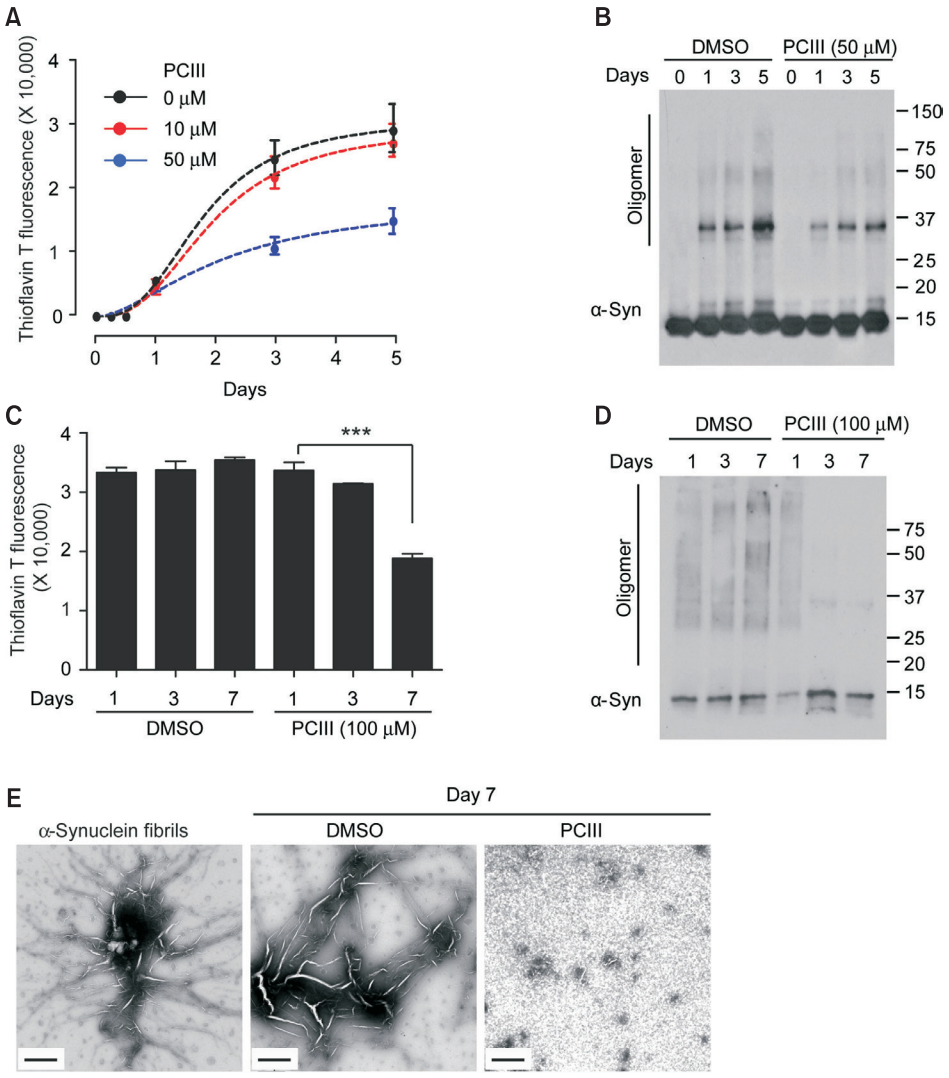

Fig. 6. PCIII inhibits α-synuclein (α-Syn) fibril formation *in vitro*. (A) Assessment of fibril formation from recombinant α-synuclein (100 μM, 100 mM sodium acetate buffer, pH 7.5) incubated in the presence or absence of PCIII (0, 10, or 50 μM) determined by thioflavin T fluorescence assay (n = 3) at the indicated time points. The fluorescence values were normalized to values at 0 day. (B) Western blots using anti-α-synuclein antibodies for α-synuclein oligomers and fibrils from the samples shown in panel A (time points: 0, 1, 3, 4 days of *in vitro* aggregation reaction). (C) Assessment of α-synuclein PFF disaggregation (50 μM, 100 mM sodium acetate buffer, pH 7.5) incubated with PCIII (100 μM) or vehicle as determined by amyloid-sensitive thioflavin T fluorescence assay (n = 3) at the indicated time points. (D) Representative western blots showing α-synuclein PFF disaggregation for the samples shown in panel C. (E) Representative transmission electron microscope images showing ultrastructure of α-synuclein oligomers and fibrils following incubation for 7 days with DMSO or 100 μM PCIII. Scale bars = 1 μm. Quantitative data are expressed as the mean ± SEM. Statistical significance was determined by ANOVA with Tukey *post-hoc* analysis. ***$P < 0.001$.

aggregation induced by 6-OHDA treatment. Effects of PCIII treatment on α-synuclein aggregation were similar to its effects on β23 aggregation.

PCIII disaggregates α-synuclein PFFs

To investigate the mechanisms by which PCIII decreased α-synuclein aggregate formation, recombinant α-synuclein was incubated in solution in the presence or absence of PCIII. Thioflavin T fluorescence, which is sensitive to amyloid fibril formation, demonstrated that the amount of α-synuclein oligomers or fibrils increased over time and reached maximum levels at approximately 4 to 5 days of incubation (Figs. 6A and 6B). Under a treatment of 10 μM PCIII, α-synuclein aggregation was slightly inhibited. Following 50 μM PCIII treatment, α-synuclein aggregation was substantially diminished. In 50 μM PCIII-added reaction, α-synuclein oligomer or fibril aggregation was only 30% of the amount accumulated in vehicle controls (Figs. 6A and 6B). These results indicate that PCIII directly affects α-synuclein aggregation processes *in vitro*.

Next, we sought to determine whether PCIII is capable of disintegrating already established α-synuclein PFFs of β-strand conformation. *In vitro* incubation of PFF with 100 μM PCIII for 7 days substantially decreased the thioflavin T fluorescence signal compared with that at the start of incubation (i.e., a 40% decrease; Fig. 6C). In contrast, *in vitro* incubation of α-synuclein PFFs (Supplementary Fig. S5A) with the DMSO control did not alter PFF stability and resulted in a slight increase of the thioflavin T fluorescence signal (Fig. 6C). To assess α-synuclein fibril species clearance, the samples used for thioflavin T assay were subjected to western blot using an anti-α-synuclein antibody. Consistent with our earlier findings, high-molecular-weight α-synuclein fibril species strongly decreased when PCIII was co-incubated with α-synuclein PFFs *in vitro* (Fig. 6D). Moreover, mixture of α-synuclein fibril and oligomers (Fig. 6E) prepared from *in vitro* incubation of recombinant human α-synuclein was subjected to *in vitro* incubation for 7 days with DMSO or PCIII. Observation of ultrastructure by transmission electron microscope revealed that PCIII disaggregates globular oligomeric structures as well as filamentous α-synuclein fibers. Taken together, these results clearly suggest that PCIII has the ability to directly interact with α-synuclein fibril and convert them into nontoxic conformations.

DISCUSSION

Here, we report the discovery of nuclear amyloid inhibitors that could serve as potential therapeutic agents for PD and other proteinopathies. The identification of several natural compounds was made possible by using a novel Tet-inducible nuclear β23 expression system. Previous studies have induced artificial β23 expression within the cytoplasm or nucleus to understand the molecular mechanisms of protein aggregate toxicity (Woerner et al., 2016). However, constitutive expression has limited applications for high-throughput screening. Synchronizing toxic protein expression and compound treatments in 96-well plates is difficult with constitutive expression. Moreover, timing concerns can compromise stable plating practices. In contrast, with the Tet-Off system, the timing of transgene expression is controlled by the addition of doxycycline. Indeed, this type of conditional gene expression system is commonly used to model toxic protein expression in cells and *in vivo* (Goverdhana et al., 2005; Lee et al., 2012). Another merit of our model is the coexpression of fluorescent reporter mCherry and nuclear β23. Tet-Off expression of β23 and mCherry allowed us to monitor nuclear β23 clearance in reference of mCherry reporter fluorescence.

There have been many studies on compounds that inhibit protein aggregation, including α-synuclein and amyloid β (Herva et al., 2014; Jha et al., 2016; Kim et al., 2010; 2015; Singh et al., 2013). Most of these studies performed *in vitro* incubation of recombinant proteins. Incubation of these proteins in solution leads to the formation of oligomers or fibrils, which can be detected quantitatively using amyloid-sensitive thioflavin T dye. With this assay system, potential protein aggregate-modifying compounds that are effective *in vivo* have been identified. However, this assay system is largely low throughput. Since producing high protein aggregates levels takes several days *in vitro*, large-scale compound screening with this system is not practical. Moreover, chemical compound instability presents additional challenges. Another weakness of this *in vitro* assay system is that the aggregation inhibitors identified may not protect cells against toxicity caused by protein aggregation. Moreover, some compounds with high potency *in vitro* may be unsuitable due to unwanted cell toxicity or undesirable pharmacokinetic properties. Even in cell culture systems, overexpression of α-synuclein itself cannot produce amyloid-like fibril formation without additional challenges like introduction of preformed α-synuclein fibrils (Volpicelli-Daley et al., 2011). However, our β23 expression system, which readily forms amyloid-like aggregates, overcomes the limitation of conventional cellular α-synuclein overexpression models. In view of these issues, our cellular model is well suited to efficiently screen large-scale compound libraries for protective agents against nuclear protein aggregation. Cell toxicity induced by nuclear β23 expression is similar to that associated with many diseases, including PD and Huntington's disease. Indeed, PCIII which has been identified as an inhibitor of β23 aggregates profoundly inhibited cellular toxicity induced by both α-synuclein and huntingtin aggregates. Although their protective mechanisms may be diverse, natural compounds that protect cells against nuclear protein aggregates can be readily assessed with Alamar blue fluorescence assay.

The nuclear β23 toxicity-inhibiting natural compounds identified in this study include PCIII, oregonin, kaempferol, and ophiocarpine. Interestingly, the chemical structure of oregonin resembles that of curcumin and its analog, which bind to α-synuclein fibrils and exert protective functions against fibril-induced toxicity (Jha et al., 2016; Singh et al., 2013). Of these compounds, PCIII was thoroughly examined due to its strong protective effects. Isothermal titration calorimetry analysis of PCIII revealed weak interaction of this compound with α-synuclein fibril (data not shown). Unfortunately, the interaction between PCIII and α-synuclein fibril seems too weak or slow to obtain thermodynamic values (over mM range of Km value) although we observed slowly increasing series of spikes of heat flow with PCIII injections. Ongoing disaggregation of fibrils into monomers in competition with compound-fibril binding might interfere with ITC measurements. More sensitive binding assays, such as surface plasmon resonance, could be applied to elucidate thermodynamic binding parameters of PCIII with diverse disease-associated amyloid aggregates. Nevertheless, relatively weak binding affinity of PCIII for α-synuclein fibril seems sufficient for disassembly of protein aggregates *in vitro* and in cells. In a similar manner, a recently reported compound exhibits very weak binding affinity to amyloid β while it exerts strong ability to degrade amyloid β aggregate and provide substantial protection in Alzheimer's disease mouse models (Kim et al., 2015). Still, it would be instrumental to synthesize derivatives of PCIII to enhance its binding affinity for protein aggregates in an attempt to further improve its therapeutic potential.

We have shown that PCIII prevents β23-, mutant huntingtin-, and α-synuclein-induced proteotoxicity by facilitating clearance of protein aggregates *in vitro* and in cells. Interestingly, PCIII markedly inhibits cytosolic and nuclear protein

aggregates, making it a potentially attractive agent for controlling protein aggregates throughout the cell and treating several neurodegenerative diseases, including Huntington's disease and PD. PCIII also has the ability to interact with established fibrils and convert them into monomers, which is an important property relevant to its potential therapeutic applications for advanced PD. Patients diagnosed with PD present motor symptoms associated with substantial loss of dopaminergic neurons (Lang and Lozano, 1998a; 1998b). Lewy body pathology is thought to begin before clinical symptoms are apparent (Lang and Lozano, 1998a; 1998b). Protein inclusions in dopaminergic neurons, which are critical for motor control, kill cells and impair cellular functions by sequestering functionally important proteins (Lee et al., 2004; Olzscha et al., 2011). Thus, compounds that disaggregate protein inclusions by eliminating α-synuclein oligomers and fibrils are more likely to improve clinical motor symptoms in patients with PD. To advance the application of PCIII for disease therapy, it will be necessary to investigate its effectiveness in appropriate animal models of PD or other neurodegenerative diseases. Unfortunately, the effect of PCIII on mouse brain function has yet to be tested. Extensive pharmacological and safety profiling must be completed before the effectiveness of PCIII in mouse models of PD and α-synuclein aggregation can be assessed. Notably, PCIII is not toxic to SH-SY5Y cells even at 100 μM doses. PCIII (1 μM) was an effective therapeutic dose that provided substantial protection against β23, mutant huntingtin and α-synuclein toxicity. Moreover, this low dose of PCIII was sufficient to consistently remove high molecular weight α-synuclein fibril species in a cellular model of PFF uptake. Interestingly, *A. decursiva* compounds that are structurally related to PCIII have been shown to readily penetrate the blood-brain barrier (Zhang et al., 2011). No overt toxicity has been profiled for extracts from *Peucedanum* species extracts (Sarkhail et al., 2013). Ultimately, PCIII has potential therapeutic applications and may provide safe treatments for brain proteinopathies. However, extensive animal studies using pure PCIII are needed.

Note: Supplementary information is available on the Molecules and Cells website (www.molcells.org).

Disclosure

The authors have no potential conflicts of interest to disclose.

ACKNOWLEDGMENTS

This research was supported by grants from the National Research Foundation of Korea (NRF-2015R1C1A1A01052708 and NRF-2017M3C7A1043848) funded by the Korea Ministry of Science, ICT, & Future Planning (MSIP). This work was supported by grants from the NIH/NINDS NS38377, NIH/NINDS NS082205, and NS098006. The authors also acknowledge the joint participation by the Adrienne Helis Malvin Medical Research Foundation and the Diana Helis Henry Medical Research Foundation through their direct engagement in the continuous active conduct of medical research in conjunction with The Johns Hopkins Hospital and the Johns Hopkins University School of Medicine and the Foundation's Parkinson's Disease Programs H-2013. We also thank Professor Jae-Byum Chang of the Sungkyunkwan University for his support in performing confocal microscope imaging.

ORCID

Sangjune Kim https://orcid.org/0000-0003-3052-3163
Hyun Sook Kwon https://orcid.org/0000-0002-8045-1543
Yun-Song Lee https://orcid.org/0000-0003-1147-8993
Heejung Choi https://orcid.org/0000-0002-1167-1526
Yunjong Lee https://orcid.org/0000-0003-0182-2279

REFERENCES

Brahmachari, S., Ge, P., Lee, S.H., Kim, D., Karuppagounder, S.S., Kumar, M., Mao, X., Shin, J.H., Lee, Y., Pletnikova, O., et al. (2016). Activation of tyrosine kinase c-Abl contributes to alpha-synuclein-induced neurodegeneration. J. Clin. Invest. *126*, 2970-2988.

Chen, I.S., Chang, C.T., Sheen, W.S., Teng, C.M., Tsai, I.L., Duh, C.Y., and Ko, F.N. (1996). Coumarins and antiplatelet aggregation constituents from Formosan Peucedanum japonicum. Phytochemistry *41*, 525-530.

Cui, L., Jeong, H., Borovecki, F., Parkhurst, C.N., Tanese, N., and Krainc, D. (2006). Transcriptional repression of PGC-1alpha by mutant huntingtin leads to mitochondrial dysfunction and neurodegeneration. Cell *127*, 59-69.

Gamen, S., Anel, A., Perez-Galan, P., Lasierra, P., Johnson, D., Pineiro, A., and Naval, J. (2000). Doxorubicin treatment activates a Z-VAD-sensitive caspase, which causes deltapsim loss, caspase-9 activity, and apoptosis in Jurkat cells. Exp. Cell Res. *258*, 223-235.

Goers, J., Manning-Bog, A.B., McCormack, A.L., Millett, I.S., Doniach, S., Di Monte, D.A., Uversky, V.N., and Fink, A.L. (2003). Nuclear localization of alpha-synuclein and its interaction with histones. Biochemistry *42*, 8465-8471.

Gorbatyuk, O.S., Li, S., Sullivan, L.F., Chen, W., Kondrikova, G., Manfredsson, F.P., Mandel, R.J., and Muzyczka, N. (2008). The phosphorylation state of Ser-129 in human alpha-synuclein determines neurodegeneration in a rat model of Parkinson disease. Proc. Natl. Acad. Sci. U. S. A. *105*, 763-768.

Goverdhana, S., Puntel, M., Xiong, W., Zirger, J.M., Barcia, C., Curtin, J.F., Soffer, E.B., Mondkar, S., King, G.D., Hu, J., et al. (2005). Regulatable gene expression systems for gene therapy applications: progress and future challenges. Mol. Ther. *12*, 189-211.

Herva, M.E., Zibaee, S., Fraser, G., Barker, R.A., Goedert, M., and Spillantini, M.G. (2014). Anti-amyloid compounds inhibit alpha-synuclein aggregation induced by protein misfolding cyclic amplification (PMCA). J. Biol. Chem. *289*, 11897-11905.

Jha, N.N., Ghosh, D., Das, S., Anoop, A., Jacob, R.S., Singh, P.K., Ayyagari, N., Namboothiri, I.N., and Maji, S.K. (2016). Effect of curcumin analogs onalpha-synuclein aggregation and cytotoxicity. Sci. Rep. *6*, 28511.

Kim, H.Y., Kim, H.V., Jo, S., Lee, C.J., Choi, S.Y., Kim, D.J., and Kim, Y. (2015). EPPS rescues hippocampus-dependent cognitive deficits in APP/PS1 mice by disaggregation of amyloid-beta oligomers and plaques. Nat. Commun. *6*, 8997.

Kim, H.Y., Kim, Y., Han, G., and Kim, D.J. (2010). Regulation of in vitro Abeta1-40 aggregation mediated by small molecules. J. Alzheimers Dis. *22*, 73-85.

Kontopoulos, E., Parvin, J.D., and Feany, M.B. (2006). Alpha-synuclein acts in the nucleus to inhibit histone acetylation and promote neurotoxicity. Hum. Mol. Genet. *15*, 3012-3023.

Landles, C. and Bates, G.P. (2004). Huntingtin and the molecular pathogenesis of Huntington's disease. Fourth in molecular medicine review series. EMBO Rep. *5*, 958-963.

Lang, A.E. and Lozano, A.M. (1998a). Parkinson's disease. First of two parts. N. Engl. J. Med. *339*, 1044-1053.

Lang, A.E. and Lozano, A.M. (1998b). Parkinson's disease. Second of two parts. N. Engl. J. Med. *339*, 1130-1143.

Lee, W.C., Yoshihara, M., and Littleton, J.T. (2004). Cytoplasmic aggregates trap polyglutamine-containing proteins and block axonal transport in a Drosophila model of Huntington's disease. Proc. Natl. Acad. Sci. U. S. A. *101*, 3224-3229.

Lee, Y., Dawson, V.L., and Dawson, T.M. (2012). Animal models of Parkinson's disease: vertebrate genetics. Cold Spring Harb. Perspect. Med. *2*, a009324.

Livak, K.J. and Schmittgen, T.D. (2001). Analysis of relative gene expression data using real-time quantitative PCR and the 2(-Delta Delta C(T)) method. Methods *25*, 402-408.

Luk, K.C., Kehm, V., Carroll, J., Zhang, B., O'Brien, P., Trojanowski, J.Q., and Lee, V.M. (2012). Pathological alpha-synuclein transmission initiates Parkinson-like neurodegeneration in nontransgenic mice. Science *338*, 949-953.

Mahul-Mellier, A.L., Fauvet, B., Gysbers, A., Dikiy, I., Oueslati, A., Georgeon, S., Lamontanara, A.J., Bisquertt, A., Eliezer, D., Masliah, E., et al. (2014). c-Abl phosphorylates alpha-synuclein and regulates its degradation: implication for alpha-synuclein clearance and contribution to the pathogenesis of Parkinson's disease. Hum. Mol. Genet. *23*, 2858-2879.

Mao, X., Ou, M.T., Karuppagounder, S.S., Kam, T.I., Yin, X., Xiong, Y., Ge, P., Umanah, G.E., Brahmachari, S., Shin, J.H., et al. (2016). Pathological alpha-synuclein transmission initiated by binding lymphocyte-activation gene 3. Science *353*, aah3374.

Masuda, M., Suzuki, N., Taniguchi, S., Oikawa, T., Nonaka, T., Iwatsubo, T., Hisanaga, S., Goedert, M., and Hasegawa, M. (2006). Small molecule inhibitors of alpha-synuclein filament assembly. Biochemistry *45*, 6085-6094.

Maynard, C.J., Bottcher, C., Ortega, Z., Smith, R., Florea, B.I., Diaz-Hernandez, M., Brundin, P., Overkleeft, H.S., Li, J.Y., Lucas, J.J., et al. (2009). Accumulation of ubiquitin conjugates in a polyglutamine disease model occurs without global ubiquitin/proteasome system impairment. Proc. Natl. Acad. Sci. U. S. A. *106*, 13986-13991.

Norris, E.H., Giasson, B.I., and Lee, V.M. (2004). Alpha-synuclein: normal function and role in neurodegenerative diseases. Curr. Top. Dev. Biol. *60*, 17-54.

Olzscha, H., Schermann, S.M., Woerner, A.C., Pinkert, S., Hecht, M.H., Tartaglia, G.G., Vendruscolo, M., Hayer-Hartl, M., Hartl, F.U., and Vabulas, R.M. (2011). Amyloid-like aggregates sequester numerous metastable proteins with essential cellular functions. Cell *144*, 67-78.

Ross, C.A. and Poirier, M.A. (2004). Protein aggregation and neurodegenerative disease. Nat. Med. *10* Suppl, S10-S17.

Rousseaux, M.W., de Haro, M., Lasagna-Reeves, C.A., De Maio, A., Park, J., Jafar-Nejad, P., Al-Ramahi, I., Sharma, A., See, L., Lu, N., et al. (2016). TRIM28 regulates the nuclear accumulation and toxicity of both alpha-synuclein and tau. Elife *5*, e19809.

Sarkhail, P., Shafiee, A., and Sarkheil, P. (2013). Biological activities and pharmacokinetics of praeruptorins from Peucedanum species: a systematic review. Biomed. Res. Int. *2013*, 343808.

Scherzinger, E., Lurz, R., Turmaine, M., Mangiarini, L., Hollenbach, B., Hasenbank, R., Bates, G.P., Davies, S.W., Lehrach, H., and Wanker, E.E. (1997). Huntingtin-encoded polyglutamine expansions form amyloid-like protein aggregates in vitro and in vivo. Cell *90*, 549-558.

Scotter, E.L., Chen, H.J., and Shaw, C.E. (2015). TDP-43 proteinopathy and ALS: insights into disease mechanisms and therapeutic targets. Neurotherapeutics *12*, 352-363.

Scotter, E.L., Vance, C., Nishimura, A.L., Lee, Y.B., Chen, H.J., Urwin, H., Sardone, V., Mitchell, J.C., Rogelj, B., Rubinsztein, D.C., et al. (2014). Differential roles of the ubiquitin proteasome system and autophagy in the clearance of soluble and aggregated TDP-43 species. J. Cell Sci. *127*, 1263-1278.

Shults, C.W. (2006). Lewy bodies. Proc. Natl. Acad. Sci. U. S. A. *103*, 1661-1668.

Singh, P.K., Kotia, V., Ghosh, D., Mohite, G.M., Kumar, A., and Maji, S.K. (2013). Curcumin modulates alpha-synuclein aggregation and toxicity. ACS Chem. Neurosci. *4*, 393-407.

Spillantini, M.G. and Goedert, M. (2000). The alpha-synucleinopathies: Parkinson's disease, dementia with Lewy bodies, and multiple system atrophy. Ann. N. Y. Acad. Sci. *920*, 16-27.

Takata, M., Shibata, S., and Okuyama, T. (1990). Structures of angular pyranocoumarins of Bai-Hua Qian-Hu, the root of peucedanum praeruptorum1. Planta Med. *56*, 307-311.

Volpicelli-Daley, L.A., Luk, K.C., Patel, T.P., Tanik, S.A., Riddle, D.M., Stieber, A., Meaney, D.F., Trojanowski, J.Q., and Lee, V.M. (2011). Exogenous alpha-synuclein fibrils induce Lewy body pathology leading to synaptic dysfunction and neuron death. Neuron *72*, 57-71.

Woerner, A.C., Frottin, F., Hornburg, D., Feng, L.R., Meissner, F., Patra, M., Tatzelt, J., Mann, M., Winklhofer, K.F., Hartl, F.U., et al. (2016). Cytoplasmic protein aggregates interfere with nucleocytoplasmic transport of protein and RNA. Science *351*, 173-176.

Wyttenbach, A., Carmichael, J., Swartz, J., Furlong, R.A., Narain, Y., Rankin, J., and Rubinsztein, D.C. (2000). Effects of heat shock, heat shock protein 40 (HDJ-2), and proteasome inhibition on protein aggregation in cellular models of Huntington's disease. Proc. Natl. Acad. Sci. U. S. A. *97*, 2898-2903.

Zhang, Z., Liu, Y.Y., Su, M.Q., Liang, X.F., Wang, W.F., and Zhu, X. (2011). Pharmacokinetics, tissue distribution and excretion study of dl-praeruptorin A of Peucedanum praeruptorum in rats by liquid chromatography tandem mass spectrometry. Phytomedicine *18*, 527-532.